International Journal of Engineering Research and Technology. ISSN 0974-3154, Volume 12, Number 12 (2019), pp. 2431-2439

Performance of Fixed-point-like Methods for a TVL1 Problem with Impulse Noise*

Yu Du Han[1] **and Jae Heon Yun**[†2]

[1]*Department of Mathematics, College of Natural Sciences, Chungbuk National University, Cheongju, Korea 28644.*
ORCID: 0000-0001-6841-8137

[2]*Department of Mathematics, Chungbuk National University, Cheongju, Korea 28644.*
ORCID: 0000-0001-6841-8137

Abstract
In this paper, we first propose a new TVL1 variational model for restoring images degraded by blurring and impulse noise, and then we propose two fixed-point-like methods, using proximal operators, for solving the new proposed TVL1 variational problem. Numerical experiments for several test images blurred by Gaussian kernel and corrupted by salt-and-pepper impulse noise are provided to demonstrate the efficiency and reliability of the fixed-point-like methods.

Keywords: TVL1 variational problems, fixed-point-like method, impulse noise, salt-and-pepper noise, proximal operator.

1991 Mathematics Subject Classification: 94A08, 54E05, 49Q20, 35M85.

1 Introduction

Image restoration which is one of the fundamental problems in image processing is to recover an original image from a given degraded image. In this paper, we consider the problem of recovering images degraded mainly by blurring and impulse noise. Two common types of impulse noise are salt-and-pepper noise and random-valued noise. Assume that the dynamic range of an image is $[d_{min}, d_{max}]$. For images corrupted by salt-and-pepper noise, the noisy pixels can take only two values d_{min} and d_{max}, while for images corrupted by random-valued noise, the noisy pixels can take any random value between d_{min} and d_{max}.

Without lose of generality, we here assume that the true image $U = (u_{ij})$ has an $N \times N$ square array and u_{ij} denotes the (i,j)-components of the image U. For convenience of exposition, the image U is represented by a long vector u of size $m = N^2$ which is defined by $u = \left(u_{*1}^T, u_{*2}^T, \ldots, u_{*N}^T\right)^T$ and $u_{*i} = (u_{1i}, u_{2i}, \ldots, u_{Ni})^T \in \mathbb{R}^N$. In this paper, an observed (or degraded) image $f \in \mathbb{R}^m$ can be represented by

$$f = Ku + \eta \tag{1.1}$$

where $K \in \mathbb{R}^{m\times m}$ is a blurring operator, $u \in \mathbb{R}^N$ is the original image, and $\eta \in \mathbb{R}^m$ denotes the impulse noise. Our objective is to restore u from the blurred and noisy image f as well as possible. The classic TVL1 model generally performs deblurring and denoising jointly or denoising purely (where K is an identity operator I) by solving the following variational problem with the l_1-norm data fidelity term and total variational regularization term

$$\min_u \left\{\|Ku - f\|_1 + \rho\|u\|_{\mathrm{TV}} : u \in \mathbb{R}^m\right\}, \tag{1.2}$$

where $\rho > 0$ is a regularization parameter and $\|u\|_{\mathrm{TV}}$ denotes the total variation (TV) of u. There are two possible definitions for $\|u\|_{\mathrm{TV}}$; one is the anisotropic TV, and the other is the isotropic TV. In this paper, we only consider the isotropic TV of $u \in \mathbb{R}^m$ which is defined by

$$\|u\|_{\mathrm{TV}} := \sum_{i=1}^{m} |(\nabla u)_i| = \sum_{i=1}^{m} \sqrt{|(\nabla_x u)_i|^2 + |(\nabla_y u)_i|^2}, \tag{1.3}$$

where the discrete gradient operator $\nabla : \mathbb{R}^m \to \mathbb{R}^{2m}$ is defined as follows:

$$(\nabla u)_i = \left((\nabla_x u)_i, (\nabla_y u)_i\right), \qquad i = 1, 2, \ldots, m$$

with

$$(\nabla_x u)_i = \begin{cases} 0 & , \text{ if } i \bmod N = 1, \\ u_i - u_{i-1}, & \text{if } i \bmod N \neq 1, \end{cases}$$

and

$$(\nabla_y u)_i = \begin{cases} 0 & , \text{ if } i \leq N, \\ u_i - u_{i-N}, & \text{if } i > N. \end{cases}$$

In recent years, much work has been done on the TVL1 model. In the light of the interesting features of the TVL1 model, it has successful applications in impulse noise removal [8, 10] and computer vision [3]. A noticeable feature of the model

*This work was supported by the National Research Foundation of Korea(NRF) funded by the Korea government(MSIT) (No. 2019R1F1A1060718), and Basic Science Research Program through the National Research Foundation of Korea(NRF) funded by the Ministry of Education(NRF-2016R1D1A1A09917364).
†Corresponding author.

is that both the l_1-norm data fidelity and regularization terms are not differentiable. This makes that finding its solutions is a challenging task both mathematically and numerically. Some algorithms for solving the TVL1 model have been developed using the proximal operator [5, 8], the primal-dual formulation [2, 4], or the augmented Lagrangian function [3].
Recently, Lu et al. [6] proposed a fixed-point algorithm for solving the following TVL1 variational problem

$$\min_u \left\{ \|Ku - f\|_1 + \lambda \|u\|_2^2 + \rho \|u\|_{\mathrm{TV}} : u \in \mathbb{R}^m \right\}, \quad (1.4)$$

where λ and ρ are positive numbers. This approach motivates us to propose the following new TVL1 variational problem

$$\min_u \left\{ \|Ku - f\|_1 + \lambda \|u\|_2 + \rho \|u\|_{\mathrm{TV}} : u \in \mathbb{R}^m \right\}. \quad (1.5)$$

Notice that the TVL1 problem (1.4) has a unique solution since its objective function is strictly convex, while the TVL1 problem (1.5) may not have a unique solution since its objective function is just convex, not strictly convex.
This paper is organized as follows. In Section 2, we provide some definitions and useful properties which we need to describe numerical algorithms for the TVL1 variational problems. In Section 3, we briefly review the fixed-point method for the TVL1 problem (1.4) proposed by Lu et al. [6]. In Section 4, we propose two fixed-point-like algorithms, using proximal operators, for solving the new proposed TVL1 variational problem (1.5). In Section 5, we provide numerical experiments for several test images blurred by Gaussian kernel and corrupted by salt-and-pepper impulse noise in order to demonstrate the efficiency and reliability of the fixed-point-like methods. Lastly we provide some concluding remarks.

2 Preliminaries

In this section, we provide some definitions and useful results which we need to develop algorithms for solving the TVL1 variational problems (1.4) and (1.5). We first provide the proximal operator introduced by Moreau [9].

Definition 2.1. Let $\psi : \mathbb{R}^m \to \mathbb{R} \cup \{+\infty\}$ be a proper, convex and lower semi-continuous (l.s.c) function. The *proximal operator* of ψ at $v \in \mathbb{R}^m$ is defined by

$$\mathrm{prox}_\psi(v) = \arg\min_u \left\{ \frac{1}{2} \parallel u - v \parallel_2^2 + \psi(u) : u \in \mathbb{R}^m \right\}. \quad (2.1)$$

Definition 2.2. Let $\psi : \mathbb{R}^m \to \mathbb{R} \cup \{+\infty\}$ be a proper, convex and l.s.c function. The *subdifferential* of ψ at $v \in \mathbb{R}^m$ is defined by

$$\partial\psi(v) = \{ y \in \mathbb{R}^m : \psi(z) \geq \psi(v) + < y, z - v >, \ \forall z \in \mathbb{R}^m \}. \quad (2.2)$$

Elements in $\partial\psi(v)$ are called *subgradeients*.

It is well-known that subdifferential of a convex function ψ is a set-valued mapping from $\mathbb{R}^m$ into a nonempty convex compact set in $\mathbb{R}^m$ (see, e.g., [1]). We now present four examples for which we can explicitly calculate the proximal operators. Note that new fixed-point-like algorithms for the TVL1 variational problem (1.5) use these proximal operators. The first example concerns the proximal operator of the absolute valued function on $\mathbb{R}$, that is, $\psi = \frac{1}{\lambda}|\cdot|$, where $\lambda > 0$.

Example 2.3. If $\lambda > 0$ and $v \in \mathbb{R}$, then

$$\mathrm{prox}_{\frac{1}{\lambda}|\cdot|}(v) = \max\left\{ |v| - \frac{1}{\lambda}, \ 0 \right\} \mathrm{sign}(v).$$

We remark that $\mathrm{prox}_{\frac{1}{\lambda}|\cdot|}$ is the well-known soft thresholding operator with $\frac{1}{\lambda}$ as the threshold, see, for example, [1]. The second example is a direct extension of the first example to $\mathbb{R}^m$.

Example 2.4. If $\lambda > 0$ and $v \in \mathbb{R}^m$, then

$$\mathrm{prox}_{\frac{1}{\lambda}\|\cdot\|_1}(v) = \max\left\{ |v| - \frac{1}{\lambda}, 0 \right\} . * \mathrm{sign}(v)$$

where $|v|$ denotes elementwise absolute value of the vector v and $.*$ denotes the elementwise multiplication.

The third example gives the proximal operator of the l_2-norm on $\mathbb{R}^m$, that is, $\psi = \frac{1}{\lambda}|| \cdot ||_2$, where $\lambda > 0$.

Example 2.5. If $\lambda > 0$ and $v \in \mathbb{R}^m$, then

$$\mathrm{prox}_{\frac{1}{\lambda}\|\cdot\|_2}(v) = \max\left\{ \|v\|_2 - \frac{1}{\lambda}, \ 0 \right\} \frac{v}{\|v\|_2}.$$

Notice that the isotropic TV of $u \in \mathbb{R}^m$ defined by (1.3) can be expressed as

$$\|u\|_{\mathrm{TV}} = (\varphi \circ B)(u), \quad (2.3)$$

where $\varphi : \mathbb{R}^{2m} \to \mathbb{R}$ is a convex function defined by

$$\varphi(v) = \sum_{i=1}^m \left\| \begin{pmatrix} v_i \\ v_{m+i} \end{pmatrix} \right\|_2 \text{ for each } v = (v_i) \in \mathbb{R}^{2m}$$

and B is a $d \times m$ matrix which represents a discrete gradient operator ∇ with $m = N^2$ and $d = 2m$. The last example gives the proximal operator of the convex function φ on $\mathbb{R}^{2m}$ which is called the generalized shrinkage formula, that is, $\psi = \frac{1}{\lambda}\varphi$, where $\lambda > 0$.

Example 2.6. If $\lambda > 0$ and $v = (v_i) \in \mathbb{R}^{2m}$, then

$$\mathrm{prox}_{\frac{1}{\lambda}\varphi}(v) = \prod_{i=1}^m \left(\mathrm{prox}_{\frac{1}{\lambda}\|\cdot\|_2} \begin{pmatrix} v_i \\ v_{m+i} \end{pmatrix} \right),$$

where $\prod$ denotes Cartesian product of vector spaces.

The following theorem outlines a relationship between the proximal operator and the subdifferential of a convex function.

Theorem 2.7 ([6, 9])**.** *If ψ is a proper, convex and l.s.c. function on $\mathbb{R}^m$ and $v \in \mathbb{R}^m$, then*

$$y \in \partial\psi(v) \qquad \Leftrightarrow \qquad v = \mathrm{prox}_\psi(v + y). \quad (2.4)$$

International Journal of Engineering Research and Technology. ISSN 0974-3154, Volume 12, Number 12 (2019), pp. 2431-2439

3 Review of Fixed-point algorithm for (1.4)

In this section, we briefly review the fixed-point method proposed in [6] for solving the TVL1 problem (1.4) which can be expressed as

$$\min_u \left\{ \|Ku - f\|_1 + \frac{\lambda}{2}\|u\|_2^2 + \rho(\varphi \circ B)(u) : u \in \mathbb{R}^m \right\}, \tag{3.1}$$

where λ and ρ are positive numbers, K is an $m \times m$ matrix, φ and B are defined the same as in (2.3).
Using Fermat rule in convex analysis for model (3.1) and relation $\partial(\varphi \circ B) = B^T \circ (\partial\varphi) \circ B$, we have

$$0 \in K^T(\partial\|\cdot\|_1)(Ku - f) + \rho B^T(\partial\varphi)(Bu) + \lambda u, \tag{3.2}$$

or equivalently

$$0 \in K^T\left(\partial\frac{1}{\lambda}\|\cdot\|_1\right)(Ku - f) + \rho B^T\left(\partial\frac{1}{\lambda}\varphi\right)(Bu) + u. \tag{3.3}$$

From relation (3.3), for any α and $\beta > 0$ we can choose a vector $a \in \partial(\frac{1}{\alpha\lambda}\|\cdot\|_1)(Ku-f)$ and a vector $b \in \partial(\frac{1}{\beta\lambda}\varphi)(Bu)$ satisfying

$$\alpha K^T a + \rho\beta B^T b + u = 0. \tag{3.4}$$

Using Theorem 2.7 and Equation (3.4), one obtains the following equations

$$a = \left(I - \operatorname{prox}_{\frac{1}{\alpha\lambda}\|\cdot\|_1}\right)(Ku - f + a), \tag{3.5}$$

$$b = \left(I - \operatorname{prox}_{\frac{1}{\beta\lambda}\varphi}\right)(Bu + b), \tag{3.6}$$

$$u = -\left(\alpha K^T a + \rho\beta B^T b\right). \tag{3.7}$$

From Equations (3.5)-(3.7), one can obtain Algorithm 1 which is similar to the fixed-point algorithm proposed in [6]. Actually, Lu et al. [6] derived the fixed-point method from relation (3.2). Numerical experiments show that Algorithm 1 using relation (3.3) performs better than the fixed-point method [6] using relation (3.2).

Algorithm 1 Fixed-point algorithm for TVL1 problem (1.4)

1: Given degraded image f, choose positive parameters $\alpha, \beta, \lambda, \rho$
2: Initialization : $u^0 = 0$, $a^0 = 0$ and $b^0 = 0$
3: **for** $k = 0$ to $maxit$ **do**
4: $\quad a^{k+1} = \left(I - \operatorname{prox}_{\frac{1}{\alpha\lambda}\|\cdot\|_1}\right)\left(Ku^k - f + a^k\right)$
5: $\quad b^{k+1} = \left(I - \operatorname{prox}_{\frac{1}{\beta\lambda}\varphi}\right)\left(Bu^k + b^k\right)$
6: $\quad u^{k+1} = -\left(\alpha K^T a^{k+1} + \rho\beta B^T b^{k+1}\right)$
7: $\quad$ **if** $\frac{\|u^{k+1}-u^k\|_2}{\|u^{k+1}\|_2} < tol$ **then**
8: $\quad\quad$ Stop
9: $\quad$ **end if**
10: **end for**

For all algorithms considered in this paper, $maxit$ denotes the maximum number of iterations and tol denotes the tolerance value of the stopping criterion.

4 Fixed-point-like algorithms for TVL1 problem (1.5)

In this section, we propose two fixed-point-like algorithms, based on the proximal operators, for solving the new proposed TVL1 variational problem (1.5). Equation (1.5) can be expressed as

$$\min_u \{\|Ku - f\|_1 + \lambda\|u\|_2 + \rho(\varphi \circ B)(u) : u \in \mathbb{R}^m\}, \tag{4.1}$$

where λ and ρ are positive numbers, φ and B are defined the same as in (2.3). Using Theorem 2.7, we can obtain the following property for the solution of TVL1 variational problem (4.1)

Theorem 4.1. *Assume that problem (4.1) has a nonzero solution u. If φ is a real-valued convex function on $\mathbb{R}^d$, B is an $d \times m$ matrix, K is an $m \times m$ matrix, and u is a nonzero solution of problem (4.1), then for any $\alpha, \beta > 0$ there exist vectors $a \in \mathbb{R}^m$ and $b \in \mathbb{R}^d$ such that*

$$a = \left(I - \operatorname{prox}_{\frac{1}{\alpha}\|\cdot\|_1}\right)(Ku - f + a), \tag{4.2}$$

$$b = \left(I - \operatorname{prox}_{\frac{\rho}{\beta}\varphi}\right)(Bu + b), \tag{4.3}$$

$$u = -\frac{\|u\|_2}{\lambda}\left(\alpha K^T a + \beta B^T b\right). \tag{4.4}$$

Conversely, if there exist $\alpha, \beta > 0, a \in \mathbb{R}^m, b \in \mathbb{R}^d$, and $u \in \mathbb{R}^m$ satisfying Equations (4.2)-(4.4), then u is a nonzero solution of TVL1 problem (4.1).

Proof. We assume that $u \in \mathbb{R}^m$ is a nonzero solution of problem (4.1). By the Fermat rule in convex analysis for model (4.1) and using the relations $\partial(\varphi \circ B) = B^T \circ (\partial\varphi) \circ B$ and $\partial(\|u\|_2) = \frac{1}{\|u\|_2}u$, we have

$$0 \in K^T(\partial\|\cdot\|_1)(Ku - f) + \rho B^T(\partial\varphi)(Bu) + \frac{\lambda}{\|u\|_2}u,$$

or equivalently

$$0 \in K^T(\partial\|\cdot\|_1)(Ku - f) + B^T(\partial\rho\varphi)(Bu) + \frac{\lambda}{\|u\|_2}u. \tag{4.5}$$

From relation (4.5), for any $\alpha, \beta > 0$ we can choose a vector $a \in \partial(\frac{1}{\alpha}\|\cdot\|_1)(Ku - f)$ and a vector $b \in \partial(\frac{\rho}{\beta}\varphi)(Bu)$ satisfying

$$\alpha K^T a + \beta B^T b + \frac{\lambda}{\|u\|_2}u = 0. \tag{4.6}$$

From (4.6), we obtain Equation (4.4). By Theorem 2.7, the inclusions $a \in \partial(\frac{1}{\alpha}\|\cdot\|_1)(Ku - f)$ and $b \in \partial(\frac{\rho}{\beta}\varphi)(Bu)$ lead to Equations (4.2) and (4.3), respectively.
Conversely, suppose that there exist $\alpha, \beta > 0$, $a, u \in \mathbb{R}^m$, and $b \in \mathbb{R}^d$ satisfying Equations (4.2)-(4.4). Again, by Theorem 2.7, Equations (4.2) and (4.3) ensure that $a \in \partial(\frac{1}{\alpha}\|\cdot\|_1)(Ku - f)$ and $b \in \partial(\frac{\rho}{\beta}\varphi)(Bu)$, respectively. Therefore, we obtain

$$\begin{aligned} 0 &= \alpha K^T a + \beta B^T b + \frac{\lambda}{\|u\|_2}u \\ &\in K^T(\partial\|\cdot\|_1)(Ku - f) + B^T(\partial\rho\varphi)(Bu) + \frac{\lambda}{\|u\|_2}u. \end{aligned}$$

Consequently, Equation (4.5) holds. Hence $u \in \mathbb{R}^m$ is a nonzero solution of TVL1 problem (4.1). □

From Equations (4.2)-(4.4) of Theorem 4.1, we can obtain fixed-point-like algorithm, called Algorithm 2, using two proximal operators for TVL1 problem (1.5).

Algorithm 2 Fixed-point-like algorithm for TVL1 problem (1.5)

1: Given degraded image f, choose positive parameters $\alpha, \beta, \lambda, \rho$
2: Initialization : $u^0 = f$, $a^0 = 0$ and $b^0 = 0$
3: **for** $k = 0$ to $maxit$ **do**
4: $\quad a^{k+1} = \left(I - \text{prox}_{\frac{1}{\alpha}\|\cdot\|_1}\right)\left(Ku^k - f + a^k\right)$
5: $\quad b^{k+1} = \left(I - \text{prox}_{\frac{\rho}{\beta}\varphi}\right)\left(Bu^k + b^k\right)$
6: $\quad u^{k+1} = -\frac{\|u^k\|_2}{\lambda}\left(\alpha K^T a^{k+1} + \beta B^T b^{k+1}\right)$
7: $\quad$ **if** $\frac{\|u^{k+1}-u^k\|_2}{\|u^{k+1}\|_2} < tol$ **then**
8: $\quad\quad$ Stop
9: $\quad$ **end if**
10: **end for**

Algorithm 2 has been developed using the explicit formula $\partial(\|u\|_2) = \frac{1}{\|u\|_2}u$ for a nonzero vector u. We next propose another fixed-point-like algorithm for TVL1 problem (4.1) which is developed without using the explicit formula for $\partial(\|u\|_2)$. Using Theorem 2.7, we can obtain the following property for the solution of TVL1 problem (4.1).

Theorem 4.2. *If φ is a real-valued convex function on $\mathbb{R}^d$, B is an $d \times m$ matrix, K is an $m \times m$ matrix, and u is a solution of problem (4.1), then for any $\alpha, \beta, \gamma > 0$ there exist vectors $a, c \in \mathbb{R}^m$ and $b \in \mathbb{R}^d$ such that*

$$a = \left(I - \text{prox}_{\frac{1}{\alpha}\|\cdot\|_1}\right)(Ku - f + a), \tag{4.7}$$

$$b = \left(I - \text{prox}_{\frac{\rho}{\beta}\varphi}\right)(Bu + b), \tag{4.8}$$

$$c = -\frac{1}{\gamma\lambda}\left(\alpha K^T a + \beta B^T b\right), \tag{4.9}$$

$$u = \text{prox}_{\frac{1}{\gamma}\|\cdot\|_2}(u + c). \tag{4.10}$$

Conversely, if there exist positive numbers α, β, γ and vectors $a, c \in \mathbb{R}^m, b \in \mathbb{R}^d$, and $u \in \mathbb{R}^m$ satisfying Equations (4.7)-(4.10), then u is a solution of TVL1 problem (4.1).

Proof. We assume that $u \in \mathbb{R}^m$ is a solution of problem (4.1). By the Fermat rule in convex analysis for problem (4.1) and using the relations $\partial(\varphi \circ B) = B^T \circ (\partial\varphi) \circ B$, we have

$$0 \in K^T(\partial\|\cdot\|_1)(Ku - f) + \rho B^T(\partial\varphi)(Bu) + \lambda(\partial\|\cdot\|_2)(u),$$

or equivalently

$$0 \in K^T(\partial\|\cdot\|_1)(Ku - f) + B^T(\partial\rho\varphi)(Bu) + \lambda(\partial\|\cdot\|_2)(u). \tag{4.11}$$

From relation (4.11), for any $\alpha, \beta, \gamma > 0$ we can choose a vector $a \in \partial(\frac{1}{\alpha}\|\cdot\|_1)(Ku - f)$, $b \in \partial(\frac{\rho}{\beta}\varphi)(Bu)$ and $c \in \partial(\frac{1}{\gamma}\|\cdot\|_2)(u)$ satisfying

$$\alpha K^T a + \beta B^T b + \gamma\lambda c = 0. \tag{4.12}$$

From Equation (4.12), we obtain Equation (4.9). By Theorem 2.7, the inclusions $a \in \partial(\frac{1}{\alpha}\|\cdot\|_1)(Ku - f)$, $b \in \partial(\frac{\rho}{\beta}\varphi)(Bu)$ and $c \in \partial(\frac{1}{\gamma}\|\cdot\|_2)(u)$ lead to Equations (4.7), (4.8) and (4.10), respectively.
Conversely, suppose that there exist $\alpha, \beta, \gamma > 0$, $a, c, u \in \mathbb{R}^m$, and $b \in \mathbb{R}^d$ satisfying Equations (4.7)-(4.10). Again, by Theorem 2.7, Equations (4.7), (4.8) and (4.10) ensure that $a \in \partial(\frac{1}{\alpha}\|\cdot\|_1)(Ku - f)$, $b \in \partial(\frac{\rho}{\beta}\varphi)(Bu)$ and $c \in \partial(\frac{1}{\gamma}\|\cdot\|_2)(u)$, respectively. From Equation (4.9), Equation (4.11) holds. Hence $u \in \mathbb{R}^m$ is a solution of TVL1 problem (4.1). □

From Equations (4.7)-(4.10) of Theorem 4.2, we can obtain another fixed-point-like algorithm, called Algorithm 3, using three proximal operators for TVL1 problem (1.5).

Algorithm 3 Fixed-point-like algorithm for TVL1 problem (1.5)

1: Given degraded image f, choose positive parameters $\alpha, \beta, \gamma, \lambda, \rho$
2: Initialization : $u^0 = 0$, $a^0 = 0$ and $b^0 = 0$
3: **for** $k = 0$ to $maxit$ **do**
4: $\quad a^{k+1} = \left(I - \text{prox}_{\frac{1}{\alpha}\|\cdot\|_1}\right)\left(Ku^k - f + a^k\right)$
5: $\quad b^{k+1} = \left(I - \text{prox}_{\frac{\rho}{\beta}\varphi}\right)\left(Bu^k + b^k\right)$
6: $\quad c^{k+1} = -\frac{1}{\gamma\lambda}\left(\alpha K^T a^{k+1} + \beta B^T b^{k+1}\right)$
7: $\quad u^{k+1} = \text{prox}_{\frac{1}{\gamma}\|\cdot\|_2}\left(u^k + c^{k+1}\right)$
8: $\quad$ **if** $\frac{\|u^{k+1}-u^k\|_2}{\|u^{k+1}\|_2} < tol$ **then**
9: $\quad\quad$ Stop
10: $\quad$ **end if**
11: **end for**

The following theorem provides convergence analysis only for Algorithm 3 since convergence for other algorithms can be analyzed similarly.

Theorem 4.3. *Let $\{a^n\}$, $\{b^n\}$, $\{c^n\}$ and $\{u^n\}$ be sequences generated by Algorithm 3. If we can find two consecutive vectors u^k and u^{k+1} such that $u^{k+1} = u^k$ for some positive values of $\alpha, \beta, \gamma, \lambda$ and ρ, then u^{k+1} is a solution of TVL1 problem (1.5).*

Proof. Substituting Equations (4.7) to (4.9) into Equation (4.10), one obtains

$$u = \text{prox}_{\frac{1}{\gamma}\|\cdot\|_2}\left(u - \frac{1}{\gamma\lambda}\left(\alpha K^T\left(I - \text{prox}_{\frac{1}{\alpha}\|\cdot\|_1}\right)(Ku - f + a) + \beta B^T\left(I - \text{prox}_{\frac{\rho}{\beta}\varphi}\right)(Bu + b)\right)\right). \tag{4.13}$$

From Theorem 4.2, it can be easily seen that if u, a and b satisfy (4.13) for some positive values of $\alpha, \beta, \gamma, \lambda$ and ρ, then u is a solution of TVL1 problem (1.5). By combining lines 4 to 7 of Algorithm 3, one obtains

$$u^{k+1} = \text{prox}_{\frac{1}{\gamma}\|\cdot\|_2}\left(u^k - \frac{1}{\gamma\lambda}\left(\alpha K^T\left(I - \text{prox}_{\frac{1}{\alpha}\|\cdot\|_1}\right)\left(Ku^k - f + a^k\right) + \beta B^T\left(I - \text{prox}_{\frac{\rho}{\beta}\varphi}\right)\left(Bu^k + b^k\right)\right)\right). \tag{4.14}$$

If $u^{k+1} = u^k$ in Equation (4.14), then u^{k+1}, a^k and b^k satisfy (4.13) for some positive values of $\alpha, \beta, \gamma, \lambda$ and ρ. Hence u^{k+1} is a solution of TVL1 problem (1.5). □

Theorem 4.3 gives an idea of how to stop the fixed-point-like algorithms. In practical applications, we do not have to find u^{k+1} which is equal to u^k. Instead, we need to find u^{k+1} which is reasonably close to u^k. Hence, for all algorithms considered in this paper we have used the following stopping criterion

$$\frac{\|u^{k+1} - u^k\|_2}{\|u^{k+1}\|_2} < tol,$$

where tol is a suitably chosen small tolerance value.

5 Numerical Experiments

In this section, we provide numerical performance results for Algorithms 1 to 3. Note that the isotropic TV of $u \in \mathbb{R}^m$ is defined by $||u||_{\mathrm{TV}} = (\varphi \circ B)(u)$, where φ and B are defined the same as in (2.3). Let D_N denote the $N \times N$ 'local difference' matrix defined by

$$D_N = \begin{pmatrix} 0 & 0 & \cdots & \cdots & 0 \\ -1 & 1 & \cdots & \cdots & 0 \\ \vdots & \ddots & \ddots & \ddots & \vdots \\ 0 & \cdots & -1 & 1 & 0 \\ 0 & \cdots & 0 & -1 & 1 \end{pmatrix}.$$

Then B can be expressed as a $d \times m$ matrix given by

$$B = \begin{pmatrix} I_N \otimes D_N \\ D_N \otimes I_N \end{pmatrix},$$

where $\otimes$ denotes the Kronecker product, I_N denotes the identity matrix of order N, $m = N^2$ and $d = 2m$.

In order to illustrate the efficiency and reliability of two fixed-point-like methods, called Algorithms 2 and 3, for solving the new proposed TVL1 problem (1.5), we provide numerical results for 4 test images such as Cameraman, Lena, House and Boat. The pixel size of 4 test images is 256×256. All numerical tests have been performed using Matlab R2018a on a personal computer with 3.6GHz CPU and 8GB RAM. $maxit$ is set to 6000 for all algorithms, and tol is set to 1×10^{-5} (for Algorithms 1 and 2) or 1.5×10^{-4} (for Algorithm 3).

To evaluate the quality of the restored images, we use the peak signal-to-noise ratio (PSNR) between the restored image and original image which is defined by

$$\text{PSNR} = 10 \log_{10} \left(\frac{N^2 \cdot \max_{i,j} |u_{i,j}|^2}{\|u - \tilde{u}\|_F^2} \right)$$

where $\| \cdot \|_F$ refers to the Frobenius norm, u and $\tilde{u}$ are the original and restored images with size $N \times N$, respectively. Also $u_{i,j}$ stands for the value of original image u at the pixel point (i, j) and N^2 is the total number of pixels. It is generally true that the larger PSNR value stands for the better quality of restored image.

For all numerical experiments, we have used the test images with an intensity range of $[0, 1]$. For all test problems, we choose the degraded test images which are resulting images blurred by Gaussian kernel of size 15×15 with reflexive boundary condition and standard deviation 9, and corrupted by 30% or 60% salt-and-pepper impulse noise. In Tables 1 and 2, P_0 represents the PSNR values for the blurred and noisy images f, Alg denotes the algorithm to be used, Cam denotes the Cameraman image, *PSNR* represents the PSNR values for the restored images, and *Iter* denotes the number of iterations. All parameters α, β, γ, λ and ρ are chosen as the best one by numerical tries,

Tables 1 and 2 provide numerical results for Algorithm 1 for TVL1 problem (1.4) and those for Algorithms 2 and 3 for TVL1 problem (1.5). Table 1 contains numerical results for degraded test images with 30% salt-and-pepper impulse noise, and Table 2 contains numerical results for degraded test images with 60% salt-and-pepper impulse noise.

In Figures 1 to 4, the first row images are true image, blurred image with 30% salt-and-pepper noise, and blurred image with 60% salt-and-pepper noise. The second row contains the images restored by Algorithms 1, 2 and 3 for blurred image with 30% salt-and-pepper noise. The third row contains the images restored by Algorithms 1, 2 and 3 for blurred image with 60% salt-and-pepper noise.

As can be seen in Tables 1 and 2, Algorithm 3 for TVL1 problem (1.5) performs best. That is, Algorithm 3 yields the highest PSNR values. Algorithm 1 for TVL1 problem (1.4) performs better than Algorithm 2 for TVL1 problem (1.5) for blurred images with 30% salt-and-pepper noise (see Table 1), while Algorithm 2 performs better than Algorithm 1 for blurred images with 60% salt-and-pepper noise (see Table 2). Both Algorithms 2 and 3 are fixed-point-like methods for solving the TVL1 problem (1.5). Numerical experiments show that Algorithm 2 using the explicit formula $\partial(\|u\|_2) = \frac{1}{\|u\|_2} u$ performs much worse than Algorithm 3 using proximal operator instead of using the explicit formula for $\partial(\|u\|_2)$.

Table 1: Numerical results for TVL1 problems with 30% salt-and-pepper impulse noise

Image	P_0	Alg	α	β	γ	λ	ρ	tol	$PSNR$	$Iter$
Cam	9.86	1	2.2	0.1		0.14	0.004	1×10^{-5}	25.12	2323
		2	0.066	0.0017		4.6	0.01	1×10^{-5}	25.56	3931
		3	6.3	0.001	1.3	1.03	0.003	1.5×10^{-4}	30.03	1843
Lena	9.92	1	2.2	0.07		0.13	0.01	1×10^{-5}	26.65	3122
		2	0.066	0.0017		4.6	0.019	1×10^{-5}	26.31	3917
		3	6.3	0.0003	1.3	1.1	0.003	1.5×10^{-4}	30.09	1845
House	9.91	1	2.2	0.2		0.15	0.02	1×10^{-5}	31.20	2195
		2	0.066	0.0017		5.0	0.026	1×10^{-5}	30.52	3363
		3	6.6	0.00003	1.3	1.1	0.003	1.5×10^{-4}	36.57	2332
Boat	9.55	1	2.2	0.06		0.14	0.007	1×10^{-5}	26.23	2907
		2	0.075	0.0009		4.8	0.026	1×10^{-5}	25.45	4843
		3	6.6	0.00008	1.3	1.1	0.003	1.5×10^{-4}	30.43	1668

Table 2: Numerical results for TVL1 problems with 60% salt-and-pepper impulse noise

Image	P_0	Alg	α	β	γ	λ	ρ	tol	$PSNR$	$Iter$
Cam	7.11	1	2.6	0.2		0.29	0.02	1×10^{-5}	22.11	1443
		2	0.063	0.0019		5.0	0.02	1×10^{-5}	23.86	3663
		3	6.3	0.002	1.1	1.1	0.014	1.5×10^{-4}	24.86	1096
Lena	7.12	1	2.6	0.2		0.29	0.03	1×10^{-5}	23.89	1716
		2	0.065	0.0014		4.8	0.032	1×10^{-5}	25.25	4275
		3	5.9	0.0008	1.1	1.1	0.015	1.5×10^{-4}	26.38	1143
House	7.07	1	2.5	0.3		0.25	0.02	1×10^{-5}	27.17	1313
		2	0.066	0.0015		5.1	0.025	1×10^{-5}	29.00	3187
		3	5.3	0.0008	0.7	1.3	0.015	1.5×10^{-4}	31.15	958
Boat	6.76	1	2.5	0.2		0.24	0.01	1×10^{-5}	23.13	1553
		2	0.065	0.001		4.7	0.02	1×10^{-5}	23.96	4330
		3	1.5	0.001	1.4	2.2	0.015	1.5×10^{-4}	24.72	1546

Figure 1: TVL1 image restoration for Cameraman image with 30% or 60% salt-and-pepper noise

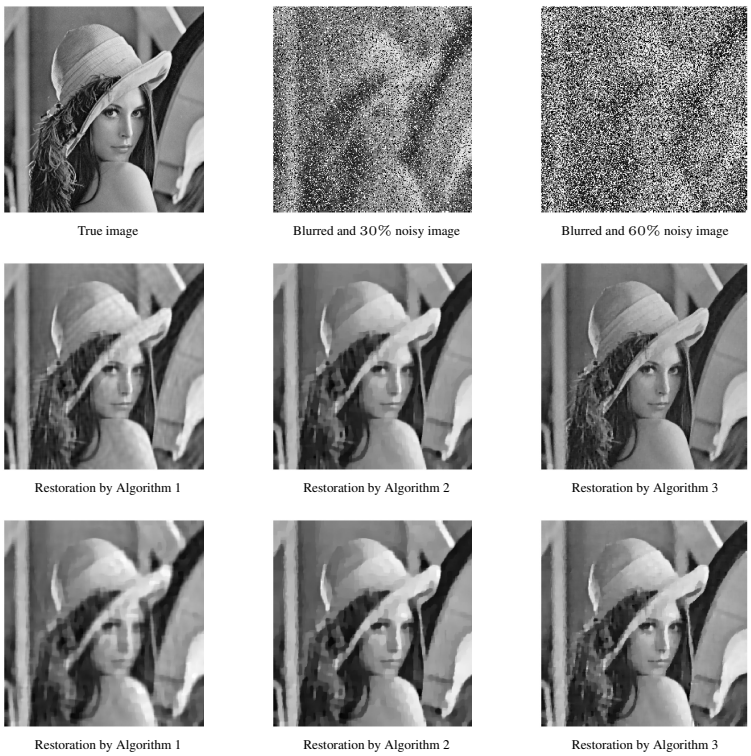

Figure 2: TVL1 image restoration for Lena image with 30% or 60% salt-and-pepper noise

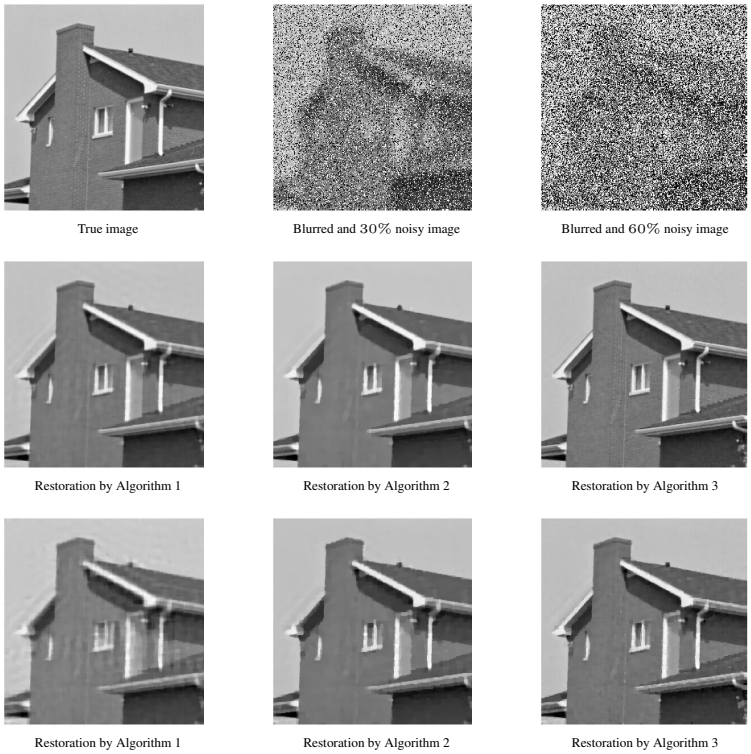

Figure 3: TVL1 image restoration for House image with 30% or 60% salt-and-pepper noise

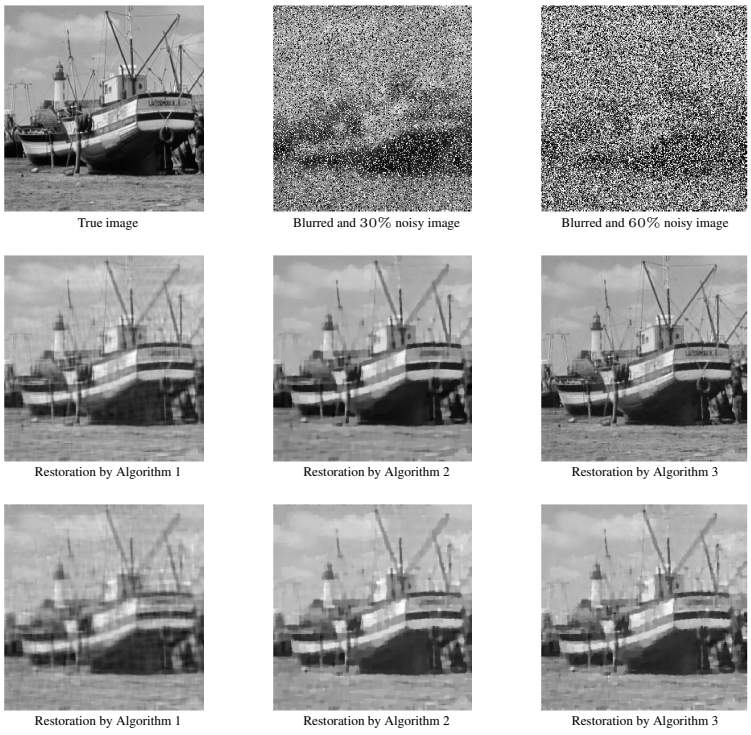

Figure 4: TVL1 image restoration for Boat image with 30% or 60% salt-and-pepper noise

6 Conclusion

In this paper, we proposed a new TVL1 variational problem (1.5) for restoring images degraded by blurring and impulse noise, and then we proposed two fixed-point-like methods, called Algorithms 2 and 3, for solving the new proposed TVL1 problem (1.5). Numerical experiments showed that Algorithm 3 without using the explicit formula $\partial(\|u\|_2) = \frac{1}{\|u\|_2}u$ performs much better than Algorithm 2 using the explicit formula for $\partial(\|u\|_2)$ and Algorithm 1 for the TVL1 problem (1.4) proposed by Lu et al. [6]. Hence, it can be concluded that the new proposed TVL1 problem (1.5) provides better quality in image restoration than the TVL1 problem (1.4), and Algorithm 3 is preferred over Algorithm 2 for the new TVL1 problem (1.5).

References

[1] A. Beck, First-order methods in optimization. SIAM, 2017.

[2] A. Chambolle and T. Pock, *A first-order primal-–dual algorithm for convex problems with applications to imaging*, J. Math. Imaging and Vision, **40** (2011), 120—145.

[3] T. Chen, W. Yin, X.S. Zhou, D. Comaniciu and T.S. Huang, *Total variation models for variable lighting face recognition*, IEEE Trans. Pattern Anal. Mach. Intell., **28** (2006), 1519-–1524.

[4] Y. Dong, M. Hintermüller and M. Neri, *An efficient primal–dual method for L1-TV image restoration*, SIAM J. Imag. Sci., **2** (2009), 1168—1189.

[5] Q. Li, C.A. Micchelli, L. Shen and Y. Xu, *A proximity algorithm accelerated by Gauss–Seidel iterations for L1/TV denoising models*, Inverse Problems, **28** (2012), Article ID 095003, p, 20.

[6] J. Lu, K. Qiao, L. Shen and Y. Zou, *Fixed-point algorithms for a TVL1 image restoration model*, Inte. J. Comp. Math., **95** (2017), 1829–1884.

[7] C.A. Micchelli, L. Shen and Y. Xu, *Proximity algorithms for image models: denoing*, Inverse Problems, **27** (2011), Article ID 045009, p, 30.

[8] C.A. Micchelli, L. Shen, Y. Xu and X. Zeng, *Proximity algorithms for the L1/TV image denoising model*, Adv. Comput. Math. **38** (2013), 401–426.

[9] J.J. Moreau, *Proximité et dualité dans un espace Hilbertien*, Bull. Soc. Math. Fr., Mém., **93** (1965), 273–299.

[10] M. Nikolova, *A variational approach to remove outliers and impulse noise*, J. Math. Imaging and Vision, **20** (2004), 99–120.

[11] L.I. Rudin, S. Osher and E. Fatemi, *Nonlinear total variation based noise removal algorithms*, Phys. D, **60** (1992), 259-268.

[12] W. Yin, D. Goldfarb and S. Osher, *The total variation regularized L1 model for multiscale decomposition*, SIAM J. Multiscale Model. Simul., **6** (2007), 190–211.